Hydrogen Chemisorption on Silica-Supported Pt Clusters: *In Situ* X-ray Absorption Spectroscopy

Scott N. Reifsnyder,[†] Mark M. Otten,[†] Dale E. Sayers,[‡] and H. Henry Lamb*,[†]

Department of Chemical Engineering, North Carolina State University, Box 7905, Raleigh, North Carolina 27695, and Department of Physics, North Carolina State University, Box 8202, Raleigh, North Carolina 27695

Received: January 16, 1997; In Final Form: April 24, 1997[⊗]

Hydrogen chemisorption on small silica-supported Pt clusters was investigated using *in situ* extended X-ray absorption fine structure (EXAFS) spectroscopy and X-ray absorption near-edge structure (XANES) spectroscopy. The clusters were found to exhibit a bulklike Pt first nearest neighbor (NN) distance (2.76 Å) and low disorder while covered by chemisorbed hydrogen. In contrast, bare Pt clusters produced by heating *in vacuo* at 300 °C are characterized by a contracted Pt NN distance (2.66 Å) and greater disorder. These effects are reversed by re-exposure of the bare Pt clusters to H_2 at 25 °C. The metal−support interface is characterized by a short Pt−O distance, irrespective of the presence of chemisorbed hydrogen. An apparent L_3 edge shift of 0.8 eV relative to bulk Pt is observed for the hydrogen-covered clusters. This shift is attributed to a decrease in the Pt L_3 edge resonance (white line) intensity, as no corresponding shift is observed at the L_2 edge. A hydrogen-related $L_{2,3}$ XANES feature at 9 eV appears with nearly equal intensity at each edge. This peak is assigned to electronic transitions from Pt 2p levels to H 1s−Pt 5d antibonding states with mixed $d_{3/2}$−$d_{5/2}$ character. From the $L_{2,3}$ XANES analysis, we find that the number of unoccupied d states in hydrogen-covered Pt clusters is 23% less than in bulk Pt. In contrast, the $L_{2,3}$ XANES spectra of bare silica-supported Pt clusters are closely similar to those of bulk Pt; quantitative analysis reveals only a slight (4%) decrease in the number of unoccupied d states.

Introduction

Supported Pt catalysts are of tremendous technological importance in a variety of applications, including petroleum naptha reforming, automobile exhaust conversion, and fine chemicals synthesis. Naptha-reforming catalysts, in particular, may contain Pt clusters containing only a few atoms on a high-surface-area alumina support.[1] Hydrogen chemisorption on Pt is central to many catalytic reactions, *e.g.,* hydrogenation and hydrogenolysis; moreover, volumetric hydrogen chemisorption is the standard technique for determining Pt dispersion, the percentage of surface-exposed Pt atoms, in supported catalysts.

In situ spectroscopic characterization of chemisorbed hydrogen on supported Pt catalysts is difficult to achieve by conventional spectroscopic techniques; however, *in situ* X-ray absorption spectroscopy (XAS) studies have identified two effects: a relaxation of Pt−Pt bonds in hydrogen-covered clusters relative to bare clusters[2,3] and an $L_{2,3}$ X-ray absorption near-edge structure (XANES) peak associated with Pt−H bonding.[4−6] The former effect explains earlier, seemingly contradictory observations of contracted nearest neighbor (NN) distances in supported clusters prepared *in vacuo* and bulklike NN distances in supported clusters prepared by hydrogen reduction of Pt ions.[7] The second effect portends the development of $L_{2,3}$ XANES as an *in situ* spectroscopic tool for monitoring hydrogen coverage under catalytic reaction conditions. Unfortunately, fundamental understanding of these effects is lacking, as there have been few reliable quantum chemical studies of Pt clusters.[8,9]

In this paper, we present an *in situ* $L_{2,3}$ edge XAS study of hydrogen chemisorption on silica-supported Pt clusters. Extended X-ray absorption fine structure (EXAFS) spectroscopy is used to determine the size and structure of the supported clusters, and the $L_{2,3}$ XANES spectra are interpreted with the aid of Hammer and Nørskov's quantum chemical model[10] of hydrogen chemisorption on late transition metal surfaces. The XANES data of bare and hydrogen-covered clusters are analyzed quantitatively to determine the number of unoccupied Pt d states.

Experimental Methods

Catalyst Preparation. Silica (Degussa Aerosil, 200 m^2/g) was washed with deionized (DI) water and dried in air at 100 °C. A 1000 ppm solution of $[Pt(NH_3)_4][NO_3]_2$ (Strem Chemicals) in DI water was added dropwise to a slurry of silica (4 g) in DI water (50 mL). After 24 h, the solid was recovered by filtration, washed with DI water, and dried in air at 100 °C. The catalyst was calcined by heating at 0.5 °C/min to 230 °C in flowing extradry O_2 (600 mL/min); the final calcination temperature was maintained for 2 h.

X-ray Absorption Spectroscopy. X-ray absorption measurements were made on beamline X-11A of the National Synchrotron Light Source at Brookhaven National Laboratory. The storage-ring energy was 2.5 GeV, and the current decayed from 250 to 110 mA during a typical fill. The beamline monochromator was equipped with a pair of Si(111) crystals for operation in the region of the Pt L_2 and L_3 edges (13.273 and 11.564 keV, respectively). Simultaneous measurements were made of the catalyst (I_0/I) and a Pt foil internal standard (I/I_{ref}) using a 5% Ar/N_2-filled ionization chamber to measure I_0 and Ar-filled ionization chambers to measure I and I_{ref}.

The Pt/SiO_2 catalysts were treated at the beamline in *in situ* cells.[11] The catalyst treatment station has been described previously.[12] The Pt/SiO_2 catalysts were dried *in vacuo* at 200 °C for 0.5 h, cooled to <50 °C, and treated in flowing H_2 at 350 °C for 1.0 h. Spectra of the freshly reduced catalysts were measured under H_2 at approximately −170 °C. After measure-

* Author to whom correspondence should be addressed. Phone: (919)-515-6395. Fax: (919)-515-3465. Email: lamb@che.ncsu.edu.
† Department of Chemical Engineering.
‡ Department of Physics.
⊗ Abstract published in *Advance ACS Abstracts,* June 1, 1997.

S1089-5647(97)00244-7 CCC: $14.00

ments, the cell was evacuated at 300 °C to remove hydrogen from the supported Pt clusters. The cell was subsequently backfilled with He at 25 °C and 1 atm prior to XAS measurements at −170 °C. The final XAS measurements were made after backfilling the cell with H_2 at 25 °C and cooling to −170 °C.

Normalized EXAFS spectra were isolated from the experimental data using standard procedures.[13] The resultant chi function was fitted in k space and r space[14] using references derived from the EXAFS spectra of Pt foil and $[Na_2Pt(OH)_6]$ measured at liquid-N_2 temperature.

The XANES spectra were isolated using a variation on the procedure described by Mansour *et al.*[15] A preliminary background removal was performed by fitting the pre-edge region (−200 to −20 eV) using the Victoreen expression and subtracting the resultant function from the data over the entire energy range. Next, the slowly oscillating background in the EXAFS region was fit using a cubic spline function. Each spectrum was normalized to the absorption edge jump measured relative to the cubic spline background at 50 eV.

In the absence of an accurate theoretical model for XANES that accounts for electronic transitions, EXAFS oscillations, and multiple-scattering events, quantitative measurements of d band occupancy must be made relative to a material with a known d band structure. In this work, a Pt foil measured at −196 °C was used as the reference material. The reference spectra were aligned with the respective $L_{2,3}$ edges (−20 to 0 eV) of the Pt foil internal standard. The reference spectra were then subtracted from the sample spectra. Thus, the energies in the resultant XANES difference spectra are calibrated relative to the inflection point of the Pt internal standard.

We used a variation of the procedure described by Mansour *et al.*[15] to determine the fractional change, f_d, in d occupancy with respect to Pt foil. The following formula is used to calculate f_d from experimental data:

$$f_d = \frac{(\Delta A_3 + 1.11\Delta A_2)}{(A_3 + 1.11A_2)_{foil}} \quad (1)$$

where

$$\Delta A_i = (A_i')_{sample} - (A_i')_{foil}$$

$$A_i' = \text{total area under the } L_i \text{ edge}$$

$$A_i = \text{"white line" peak area at the } L_i \text{ edge}$$

The ΔA_i values are the normalized areas attributed to electronic transitions to unoccupied d states in the XANES difference spectra. The A_i values are difficult to determine directly due to the necessity of separating the contributions of electronic transitions to unoccupied d states and to the continuum. However, the denominator $(A_3 + 1.11A_2)$ can be estimated for Pt foil by taking the difference between the L_3 and L_2 XANES spectra and assuming that the bulk ratio of $^5/_2$ to $^3/_2$ d holes is 14.[15,16]

Results

The Pt L_3 edge EXAFS spectrum of a 1 wt % Pt/SiO_2 catalyst after reduction in H_2 at 350 °C is shown in Figure 1a; the signal-to-noise ratio is sufficient to permit data analysis over a wide k range ($3.1 < k < 14.4$ Å^{-1}). A Pt−Pt phase-corrected Fourier transform (Figure 1b) reveals a prominent Pt first-shell peak; however, peaks arising from the second and third shells of the fcc structure (whose expected positions are indicated by arrows in Figure 1b) are either very weak or absent. The first-shell contribution was fit in r space ($1.5 < r < 3.7$ Å) using a Pt foil reference. The results (Table 1) evidence that the catalyst contains small Pt clusters characterized by a Pt NN distance equivalent to that of the bulk metal (2.77 Å).

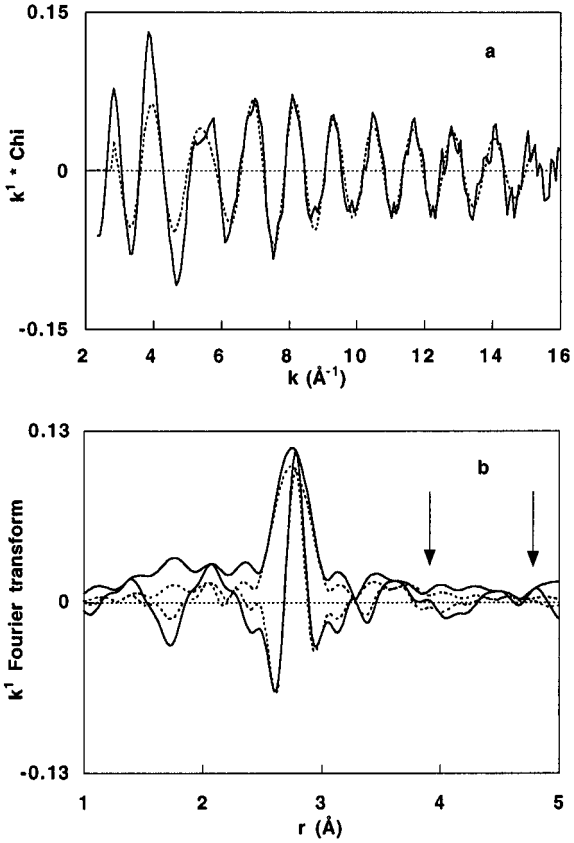

Figure 1. Pt L_3 EXAFS data (solid line) and calculated Pt−Pt fit (dashed line) in k and r space for 1 wt % Pt/SiO_2 reduced at 350 °C: (a) k^1-weighted chi function and (b) k^1-weighted Pt−Pt phase-corrected Fourier transform. The arrows indicate the expected position of higher Pt shells.

TABLE 1: Pt L_3 Edge EXAFS Results

sample/treatments	backscatterer	N^a	R^b (Å)	$(\Delta\sigma^2)^c$ (Å^2)	ΔE_0 (eV)
1% Pt/SiO_2					
350 °C H_2	Pt	5.4	2.76	0.0031	2.8
	O	1.9	2.05	0.026	−7.2
350 °C H_2; 300 °C Vac	Pt	5.0	2.66	0.0048	3.6
	O	1.4	2.03	0.027	−8.3
350 °C H_2; 300 °C Vac; H_2	Pt	5.5	2.76	0.0033	2.0
	O	1.9	2.06	0.025	−8.0
2% Pt/SiO_2					
350 °C H_2	Pt	7.7	2.77	0.0025	1.0
	O	1.5	2.07	0.025	−7.8

[a] Coordination number (±15%). [b] Interatomic distance (±0.01 Å). [c] Relative Debye−Waller factor (±15%).

Comparisons of the experimental and calculated EXAFS functions in k and r space are shown in Figure 1. The Pt−Pt contribution fits the data well in the high-k region, but significant deviations between the calculated EXAFS and the data are apparent for $k < 6$ Å^{-1}. A k^1-weighted Fourier transform (Figure 1b), which emphasizes the low-k region, shows deviations primarily on the low-r side of the Pt−Pt peak. Under the assumption that the EXAFS spectrum contained additional contributions from low-Z backscatterers, a k-space difference spectrum was created by subtracting the Pt−Pt contribution from the data. The difference spectrum was fit successfully using a

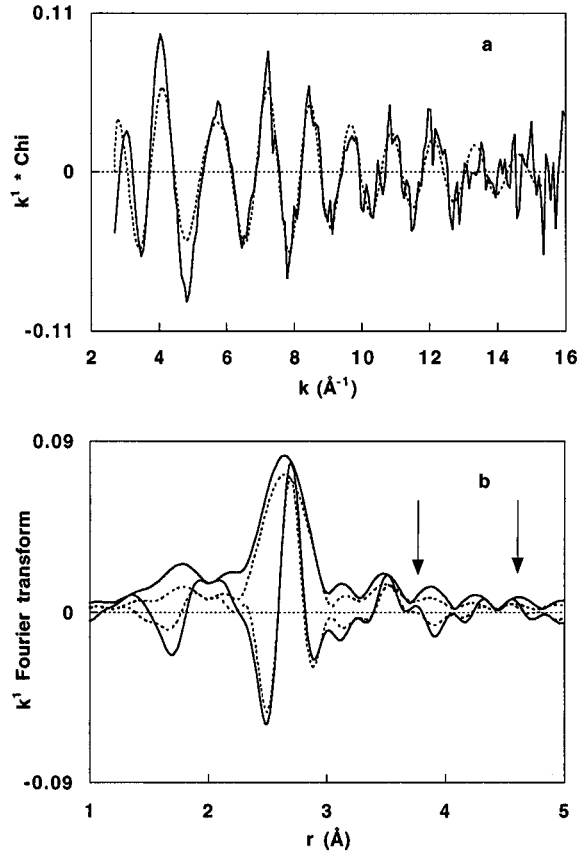

Figure 2. Pt L_3 first-shell EXAFS data (solid line) and calculated Pt−Pt fit (dashed line) in k and r space for 1 wt % Pt/SiO_2 reduced at 350 °C and subsequently evacuated at 300 °C: (a) k^1-weighted chi function and (b) k^1-weighted Pt−Pt phase-corrected Fourier transform. The arrows indicate the expected position of higher Pt shells.

short Pt−O contribution; however, a large Debye−Waller factor and significant inner potential correction are required (Table 1).

The Pt L_3 EXAFS spectrum of the 1 wt % Pt/SiO_2 catalyst after reduction and subsequent evacuation at 300 °C is shown in Figure 2a. In comparison to the spectrum of the freshly reduced catalyst, the EXAFS amplitude is smaller, especially at high k. The first-shell Pt−Pt peak in the phase-corrected Fourier transform ($3.3 < k < 12.1$ Å^{-1}) (Figure 2b) is smaller in magnitude, broader, and shifted toward lower r values; higher shell Pt−Pt peaks are absent. The EXAFS spectrum was fit in r space ($1.5 < r < 3.7$ Å), and comparisons of the experimental and calculated EXAFS functions in k and r space are presented in Figure 2. The results (Table 1) indicate that evacuation does not significantly alter the Pt−Pt coordination number, but results in a large contraction of the Pt NN distance. There is a concomitant increase in disorder, as evidenced by the larger Debye−Waller factor. The difference spectrum obtained by subtracting the Pt−Pt contribution from the data is closely similar to that found for the freshly reduced catalyst. The fit (Table 1) evidences reductions in the Pt−O coordination number and distance.

The Pt L_3 EXAFS spectrum of the catalyst after re-exposure to H_2 at 25 °C is indistinguishable from that of the freshly reduced catalyst. The EXAFS parameters derived from an r-space fit ($3.3 < k < 13.9$ Å^{-1}, $1.5 < r < 3.7$ Å) are given in Table 1. The results demonstrate that after hydrogen chemisorption the Pt clusters have returned to the same physical state observed immediately after reduction.

The EXAFS parameters of Pt crystallites formed by reduction of a 2 wt % Pt/SiO_2 catalyst in H_2 at 350 °C are given in Table 1. By comparison, the Pt NN distance and Debye−Waller factor are similar to those observed for the freshly reduced 1 wt % Pt/SiO_2 catalyst; however, the first-shell coordination number is much larger, indicating the formation of larger particles. Moreover, the second, third, and fourth Pt−Pt shells are evident in the radial structure function (not shown). The observation of a distinct second-shell peak arising from the (111)-interplanar distance in the fcc structure evidences that the particles are three-dimensional crystallites. The difference spectrum obtained by subtracting the Pt−Pt contribution from the data is similar to that found for the freshly reduced 1 wt % Pt catalyst. The fitting results (Table 1) reveal that the Pt−O coordination number is smaller for the 2 wt % Pt/SiO_2 catalyst.

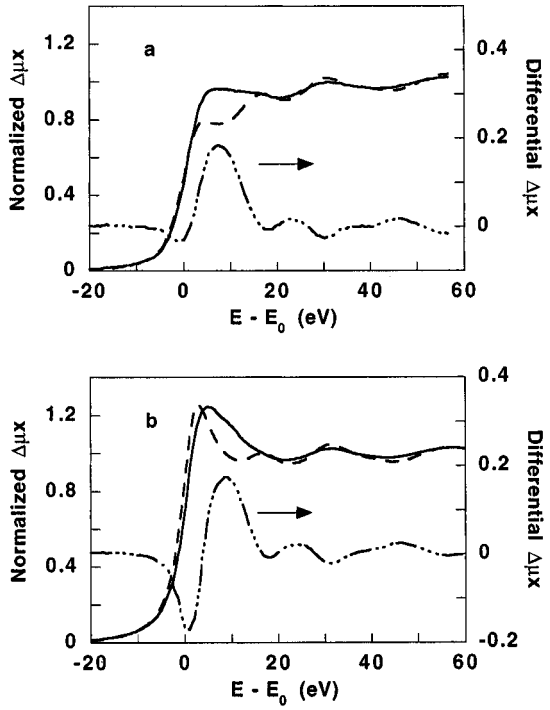

Figure 3. Normalized Pt L_2 (a) and L_3 (b) XANES spectra for 1 wt % Pt/SiO_2 reduced at 350 °C (solid line), Pt foil reference (dashed line), and the difference (dash-dot line).

The normalized $L_{2,3}$ XANES spectra of the freshly reduced 1 wt % Pt/SiO_2 catalyst and a Pt foil reference are compared in Figure 3. The L_3 absorption edge of the hydrogen-covered clusters exhibits a shift to higher energy relative to the reference, but the L_2 absorption edge does not. The *apparent* threshold energy shifts measured at each edge are given in Table 2. Difference spectra were obtained by subtracting the reference spectrum from that of the sample at each edge. The L_2 difference spectrum (Figure 3a) contains a very weak negative feature near the edge and a strong positive peak at 9 eV relative energy. The L_3 difference spectrum (Figure 3b) contains a similar positive peak at 9 eV and a medium-intensity negative peak near the edge. Structure-related features are observed in each difference spectrum at 20−50 eV.

The normalized Pt $L_{2,3}$ XANES spectra of the evacuated catalyst and a Pt foil reference are compared in Figure 4. Neither the L_2 nor the L_3 absorption edge of the evacuated catalyst exhibits a substantial energy shift relative to the foil (Table 2). The Pt L_3 white line intensity of the bare clusters is reduced relative to that of the foil, giving rise to a sharp negative difference feature (Figure 4b). The 9-eV peak observed in the $L_{2,3}$ difference spectra of the freshly reduced catalyst has diminished in intensity and is comparable to the structure-related features at 20−50 eV.

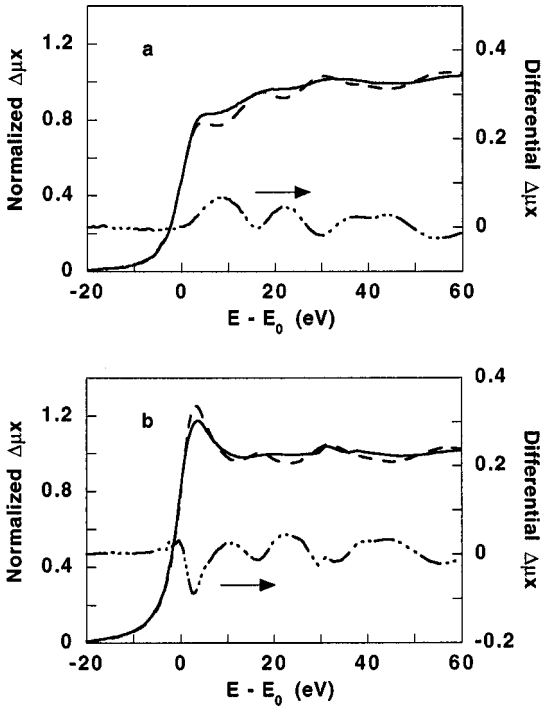

Figure 4. Normalized Pt L_2 (a) and L_3 (b) XANES spectra for 1 wt % Pt/SiO_2 reduced at 350 °C and subsequently evacuated at 300 °C (solid line), Pt foil reference (dashed line), and the difference (dash-dot line).

Difference spectra were also obtained by subtracting the $L_{2,3}$ XANES spectra of the bare Pt clusters from those of the hydrogen-covered Pt clusters. A positive peak at 9 eV is observed in both the L_2 and L_3 difference spectra (Figure 5), and a strong negative peak is observed near the L_3 edge. Thus, the spectra are qualitatively similar to those in Figure 3. Closely similar difference spectra are obtained for hydrogen-covered Pt clusters in the freshly reduced catalyst and in the evacuated catalyst after subsequent re-exposure to H_2 at 25 °C.

Discussion

EXAFS spectroscopy of Pt/SiO_2 catalysts demonstrates that the structure of hydrogen-covered supported Pt aggregates is bulklike and insensitive to particle size. This is evidenced by bulk-equivalent Pt NN distances and small relative Debye−Waller factors in hydrogen-covered Pt clusters and Pt crystallites supported on SiO_2. On the basis of the first-shell Pt−Pt coordination numbers, we estimate nuclearities of *ca.* 14 and 80 atoms, respectively, for the clusters and crystallites using a truncated octahedron model. The estimated dispersions of 1.0 and 0.85 are in good agreement with H/Pt ratios obtained from the empirical correlation of Kip *et al.*[17] The appearance of second, third, and fourth shells in the radial structure function indicates that the Pt crystallites have three-dimensional fcc structures. The observation that small hydrogen-covered Pt clusters adopt bulklike structures is consistent with previous EXAFS results for highly dispersed supported metal catalysts.[1,18−23]

Hydrogen desorption from silica-supported Pt clusters occurs by heating *in vacuo* at temperatures > 150 °C.[22] Our results indicate that evacuation at 300 °C to desorb hydrogen does not alter the Pt cluster nuclearity; however, the Pt NN distance contracts markedly, and there is a concomitant increase in disorder. These changes are clearly associated with hydrogen desorption, as they are reversed by re-exposure of the bare clusters to H_2 at 25 °C. The NN distance contraction (0.10 Å) is larger than typically reported for bare zeolite-supported clusters of a similar size,[24] but equivalent to that found for bare Pt clusters on γ-Al_2O_3.[3]

Apparent contractions of NN distances in metal clusters, as determined by EXAFS spectroscopy, can be artifacts of anharmonic, *i.e.*, non-Gaussian, disorder which is not accounted for in the standard EXAFS equation.[25−27] Anharmonicity arises from asymmetry of the pair distribution function and includes static and dynamical contributions. Neglect of anharmonic disorder can result in large errors, including apparent reductions in coordination number and NN distance.[27,28] Errors arising from dynamical asymmetric effects can be minimized by low-temperature measurements, such as those reported herein; however, static contributions can be significant, especially for small clusters. Fortunately, a recent EXAFS analysis of bare Pt clusters in Y zeolite showed that static asymmetry of the pair distribution function could be neglected without introducing significant errors.[24] Thus, we suggest that the 2.66 Å NN distance is intrinsic to bare silica-supported Pt clusters.

The structure of the metal−support interface in highly dispersed supported metal catalysts has been investigated extensively by EXAFS spectroscopy using the difference file technique.[1,19,21−23,29,30] The present results (Table 1) indicate the presence of O backscatterers at a short distance from the Pt atoms in the freshly reduced 1% Pt/SiO_2 catalyst. A similar short Pt−O distance was found by Lytle *et al.* in an earlier EXAFS investigation of Pt/SiO_2 catalysts.[31] The measured Pt−O coordination number is in good agreement with the theoretical value for three-dimensional Pt clusters having a Pt−Pt coordination number of 5.5 and three support oxygen atoms (ligands) coordinating each interfacial Pt atom.[29] The large disorder in the Pt−O interfacial distance, as evidenced by the Debye−Waller factor, is likely due to the amorphous nature of the silica support. A similar albeit smaller Pt−O contribution was found for the freshly reduced 2 wt % Pt/SiO_2 catalyst (Table 1). The short Pt−O distance observed in highly dispersed Pt/SiO_2 catalysts suggests that the Pt atoms at the metal−support interface are polarized and bear a partial positive charge.[1]

Desorption of H_2 from the supported Pt clusters leads to reversible changes in the structure of the metal−support interface. A significant decrease in the Pt−O coordination number and a small decrease in the Pt−O distance are observed after heating the freshly reduced 1 wt % Pt/SiO_2 catalyst *in vacuo* at 300 °C (Table 1). As the Pt−Pt coordination number does not change significantly, we infer that the percentage of Pt atoms at the metal−support interface remains approximately constant; therefore, the results are consistent with a decrease from 3 to 2 in the average number of support oxygen atoms (ligands) coordinating each interfacial Pt atom. These effects correlate with the observed contraction of the Pt−Pt NN distance, and they are reversed by re-exposure of the bare clusters to H_2 at 25 °C.

A supported Pt cluster is not expected to exhibit the same electronic structure as bulk Pt due to intrinsic size effects, metal−support interactions, and adsorbate bonding interactions. $L_{2,3}$ XANES spectroscopy provides information on the binding energies of 2p electrons relative to the Fermi level (E_F) and on the unoccupied d density of states (DOS) near E_F. The unoccupied d DOS is reflected in the intensities of the $2p \rightarrow 5d$ edge resonances (white lines). The L_3 white line ($2p_{3/2}$ initial state) probes the total ($d_{3/2} + d_{5/2}$) unoccupied d DOS, and the L_2 white line ($2p_{1/2}$ initial state) probes only the unoccupied $d_{3/2}$ states, as a consequence of the dipole selection rule ($\Delta J = 0, \pm 1$).[15] Due to spin−orbit coupling, the unoccupied d state in an isolated Pt atom is $d_{5/2}$, and notwithstanding broadening within the band, the d holes near E_F in bulk Pt have predomi-

TABLE 2: Pt $L_{2,3}$ XANES Results

	L_2 edge			L_3 edge			
sample/treatments	ΔE^a	ΔA^-	ΔA^+	ΔE^a	ΔA^-	ΔA^+	$f_d{}^b$
1% Pt/SiO_2							
350 °C H_2	0.2	−0.46	1.95	0.8	−1.51	1.92	−0.23
350 °C H_2; 300 °C Vac	0.0	0.00	0.60	−0.1	−0.34	0.17	−0.04
350 °C H_2; 300 °C Vac; H_2	0.0	−0.27	1.76	0.8	−1.55	1.90	−0.22
2% Pt/SiO_2							
350 °C H_2				0.2	−0.58	1.01	−0.08[c]

[a] $\Delta E = E_{Pt/SiO_2} - E_{Pt\ foil}$ (±0.2 eV). [b] Fractional excess of unoccupied d states relative to Pt foil, calculated using eq 1. [c] Estimated assuming $\Delta A^-(L_2) = 0$; actual value will be slightly more negative.

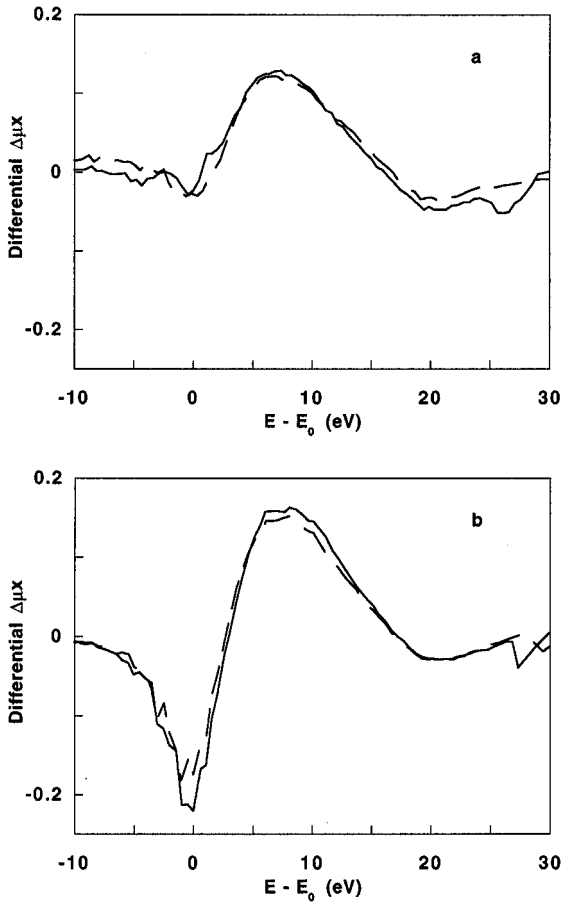

Figure 5. Normalized Pt L_2 (a) and L_3 (b) XANES difference spectra for 1 wt % Pt/SiO_2 obtained by subtracting spectra of the catalyst after evacuation at 300 °C from the corresponding spectra of the catalyst after reduction at 350 °C (solid line) and after re-exposure to H_2 at 25 °C subsequent to evacuation at 300 °C (dashed line).

nantly $d_{5/2}$ character.[16] As a result, chemical effects on Pt d occupancy are expected to affect the L_3 white line more strongly than the L_2 white line.[15]

XANES spectra can be difficult to interpret owing to superposition of the continuum absorption threshold and the edge resonances.[15] This is especially true for Pt L_3 XANES spectra because of the large Pt 2p → 5d white line intensity. Conversely, the lack of a substantial white line makes the Pt L_2 edge energy a good measure of the continuum absorption threshold. Because the L_2 and L_3 edges are associated with 2p electronic excitations, charge transfer and size-related core-level shifts should have the same effect on the continuum threshold at each edge. As there are no detectable L_2 edge energy differences between the Pt cluster catalysts and Pt foil (Table 2), we infer that any electronic effects on the 2p core levels are small (<0.2 eV). Consequently, the L_3 edge shift observed for hydrogen-covered Pt clusters must be attributed to changes in the edge resonance(s).

The $L_{2,3}$ XANES difference spectra in Figure 4 allow us to assess the unoccupied d DOS of bare Pt clusters with respect to Pt foil. The sharp negative feature near the L_3 edge indicates a decrease in the number of unoccupied d states near E_F. The absence of a similar feature at the L_2 edge indicates that an overwhelming majority of the unoccupied Pt d states are $d_{5/2}$. The decease in the number of unoccupied d states near E_F can be interpreted as a narrowing of the d band, which has been experimentally verified for small metal clusters on inert supports using photoemission techniques.[32] Narrowing of the d band is expected due to the low coordination numbers of Pt atoms in small clusters. Quantitatively, the change amounts to a 4% decrease ($f_d = -0.04$) in the number of unoccupied d states. Broader features that appear at higher energies in the L_2 and L_3 XANES difference spectra of the bare clusters arise from structural differences primarily involving the higher coordination shells.[7]

The L_2 and L_3 XANES difference spectra of hydrogen-covered Pt clusters (Figure 3) contain similar features at 9 eV above the edge. Samant and Boudart,[4] who studied the Pt L_3 XANES of bare and hydrogen-covered Pt clusters in Y zeolite, proposed that the 9-eV peak arises from a transition of $2p_{3/2}$ electrons to unoccupied Pt−H antibonding states.[4] A similar interpretation of the $L_{2,3}$ XANES of Pt clusters in hydrogen Y zeolite was put forward by Boyanov and Morrison.[33] Asakura *et al*. discounted the original assignment to unoccupied Pt−H antibonding states, suggesting instead assignment of this Pt−H XANES feature to a continuum resonance.[6] The negative $L_{2,3}$ difference features indicate a substantial reduction in L_3 white line intensity and a much smaller reduction in L_2 white line intensity relative to Pt foil. On this basis, we conclude that hydrogen chemisorption on supported Pt clusters leads to a reduction in the number of unoccupied d states. The different magnitudes of the effects at the L_2 and L_3 edges attest to the prevalence of $d_{5/2}$ unoccupied states near E_F. Moreover, the experimental L_3 edge shift (Table 2) is seen to originate from a reduction in white line intensity and not from a shift in the continuum X-ray absorption threshold.

The difference spectra in Figure 5 were created using the $L_{2,3}$ XANES spectra of the bare Pt clusters as references, thereby minimizing potential artifacts arising from different Pt−Pt coordination numbers. The resultant spectra are closely similar to those in Figure 3. Moreover, the effects of chemisorbed hydrogen on the Pt $L_{2,3}$ XANES are seen to be reversible and highly reproducible. Asakura *et al.* found that the intensity of the 9-eV feature in such difference spectra correlated with the H/Pt ratio for Pt particles on a variety of supports.[6]

Molecular orbital theory predicts that when a hydrogen atom interacts with a transition metal surface, a M−H bonding state forms below the d band and a M−H antibonding state forms above the Fermi level.[34,35] The adsorbate-induced bonding state is broadened by interaction with the metal s band, and the antibonding state is broadened extensively by interactions with metal continuum states. Hammer and Nørskov[10] demonstrated

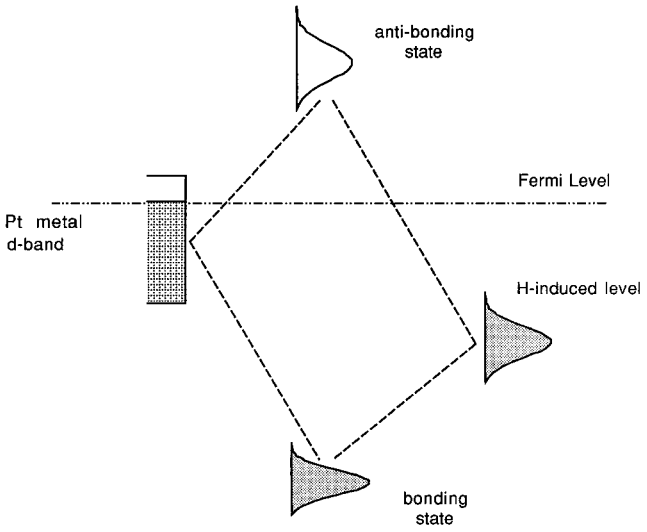

Figure 6. Illustration of the bonding interactions between a Pt surface and a hydrogen atom.[10]

through density functional theory calculations that coupling between the s-like bonding state and the metal d band leads to further stabilization of the bonding state and creation of an s−d antibonding state just above the metal d band (Figure 6). For metals like Ni and Pt with unfilled d bands, this state will be pushed above E_F and hence remain empty. An important consequence of s−d coupling is that it lends d character to the M−H antibonding states. Metal−hydrogen bonding is also expected to stabilize the d states,[35] and this effect is expected to be significant in metal clusters since virtually all atoms are at the surface.

These quantum chemical concepts can be used to interpret the $L_{2,3}$ XANES spectra of hydrogen-covered Pt clusters. The 9-eV feature is assigned to the H 1s−Pt 5d antibonding level, which is broadened due to interactions with continuum states. We infer that the Pt−H antibonding states have mixed $d_{3/2}$−$d_{5/2}$ character, since the 9-eV peak appears with nearly equal intensity at each edge. For reasons that are as yet unclear, the antibonding level appears at higher energy relative to E_F than predicted by Hammer and Nørskov's model. Stabilization of the Pt cluster d orbitals results in fewer unoccupied d states near E_F. Consequently, the 2p to 5d transition probability decreases, and the L_3 white line intensity is reduced. Since the $d_{5/2}$ states dominate near E_F, the effect is most pronounced at the L_3 edge.

To obtain a quantitative estimate of the changes in Pt d electronic structure induced by hydrogen chemisorption, we deconvoluted the difference spectra in Figure 3 by fitting the negative (white line) peak with a Lorentzian function and the positive 9-eV peak with a Gaussian function. As can be seen in Table 2, there is good agreement between the 9-eV peak areas (ΔA^+) determined at each edge. This area should be proportional to the H/Pt ratio,[6] and the hydrogen-covered Pt crystallites in the 2 wt % catalyst exhibit a smaller ΔA^+ (Table 2) than the hydrogen-covered Pt clusters, consistent with this expectation. The negative peak areas (ΔA^-) were used to estimate the fractional excess of unoccupied d states (f_d) relative to bulk Pt, using the method of Mansour *et al.*[15] The f_d values are given in Table 2. For the hydrogen-covered Pt clusters, there are 23% fewer unoccupied d states than in bulk Pt. The less negative f_d value found for the hydrogen-covered Pt crystallites indicates that as particle size increases, chemisorbed hydrogen has a smaller effect on Pt electronic structure, as expected.

In conclusion, significant changes in Pt−Pt bonding and cluster electronic structure occur concomitant with hydrogen chemisorption on silica-supported Pt clusters. A fuller understanding of these effects awaits the results of accurate quantum chemical calculations on Pt clusters.

Acknowledgment. The authors gratefully acknowledge the contributions of B. Boyanov and D. C. Koningsberger to this work, and we thank the staff of beamline X-11 of the National Synchrotron Light Source for their assistance. This work was supported by an NSF Presidential Young Investigator Award (CTS-8958350). In addition, SNR acknowledges financial assistance in the form of a Ph.D. fellowship from Hoechst-Celanese Corporation.

References and Notes

(1) Gates, B. C.; Koningsberger, D. C. *CHEMTECH* **1992**, *22*, 300.
(2) Moraweck, B.; Clugnet, G.; Renouprez, A. J. *Surf. Sci. Lett.* **1979**, *81*, L631.
(3) Vaarkamp, M. Doctoral Thesis, Eindhoven University of Technology, The Netherlands, 1993.
(4) Samant, M. G.; Boudart, M. *J. Phys. Chem.* **1991**, *95*, 4070.
(5) Ichikuni, N.; Iwasawa, Y. *Catal. Lett.* **1993**, *20*, 87.
(6) Asakura, K.; Kubota, T.; Ichikuni, N.; Iwasawa, Y. *Stud. Surf. Sci. Catal.* **1996**, *101*, 911.
(7) Balerna, A.; Bernieri, E.; Picozzi, P.; Reale, A.; Santucci, S.; Burattini, E.; Mobilio, S. *Phys. Rev. B* **1985**, *31*, 5058.
(8) Cheng, H.-P.; Ellis, D. E. *J. Chem. Phys.* **1991**, *94*, 3735.
(9) Ellis, D. E.; Guo, J.; Cheng, H.-P.; Low, J. J. *Adv. Quantum Chem.* **1991**, *22*, 125.
(10) Hammer, B.; Nørskov, J. K. *Nature* **1995**, *376*, 238.
(11) Kampers, F. W. H.; Maas, T. M. J.; van Grondelle, J.; Brinkgreve, P.; Koningsberger, D. C. *Rev. Sci. Instrum.* **1989**, *60*, 2635.
(12) Reifsnyder, S. N.; Lamb, H. H. *Catal. Lett.* **1996**, *40*, 155.
(13) Sayers, D. E.; Bunker, B. A. In *X-Ray Absorption: Principles, Applications, Techniques of EXAFS, SEXAFS, and XANES*; Koningsberger, D. C., Prins, R., Eds.; John Wiley & Sons: New York, 1988; p 211.
(14) Vaarkamp, M.; Linders, J. C.; Koningsberger, D. C. *Physica B* **1995**, *208 & 209*, 159.
(15) Mansour, A. N.; Cook, J. W., Jr.; Sayers, D. E. *J. Phys. Chem.* **1984**, *88*, 2330.
(16) Brown, M.; Peierls, R. E.; Stern, E. A. *Phys. Rev. B* **1977**, *15*, 738.
(17) Kip, B. J.; Duivenvoorden, F. B. M.; Koningsberger, D. C.; Prins, R. *J. Catal.* **1987**, *105*, 26.
(18) Via, G. H.; Sinfelt, J. H.; Lytle, F. W. *J. Chem. Phys.* **1979**, *71*, 690.
(19) Lagarde, P.; Murata, T.; Vlaic, B.; Freund, E.; Dexpert, H.; Bournonville, J. P. *J. Catal.* **1983**, *84*, 333.
(20) van't Blik, H. F. J.; van Zon, J. B. A. D.; Huizinga, T.; Vis, J. C.; Koningsberger, D. C.; Prins, R. *J. Am. Chem. Soc.* **1985**, *107*, 3139.
(21) Chang, J.-R.; Koningsberger, D. C.; Gates, B. C. *J. Am. Chem. Soc.* **1992**, *114*, 6460.
(22) Miller, J. T.; Meyers, B. L.; Modica, F. S.; Lane, G. S.; Vaarkamp, M.; Koningsberger, D. C. *J. Catal.* **1993**, *143*, 395.
(23) Purnell, S. K.; Sanchez, K. M.; Patrini, R.; Chang, J. R.; Gates, B. C. *J. Phys. Chem.* **1994**, *98*, 1205.
(24) Boyanov, B. I.; Morrison, T. I. *J. Phys. Chem.* **1996**, *100*, 16310.
(25) Eisenberger, P.; Brown, G. S. *Solid State Commun.* **1979**, *29*, 481.
(26) Marques, E. C.; Sandstrom, D. R.; Lytle, F. W.; Greegor, R. B. *J. Chem. Phys.* **1982**, *77*, 1027.
(27) Hansen, L. B.; Stoltze, P.; Nørskov, J. K.; Clausen, B. S.; Niemann, W. *Phys. Rev. Lett.* **1990**, *64*, 3155.
(28) Clausen, B. S.; Gråbæk, L.; Topsøe, H.; Hansen, L. B.; Stoltze, P.; Nørskov, J. K.; Nielsen, O. H. *J. Catal.* **1993**, *141*, 368.
(29) van Zon, J. B. A. D.; Koningsberger, D. C.; van't Blik, H. F. J.; Sayers, D. E. *J. Chem. Phys.* **1985**, *82*, 5742.
(30) Moller, K.; Koningsberger, D. C.; Bein, T. *J. Phys. Chem.* **1989**, *93*, 6116.
(31) Lytle, F. W.; Greegor, R. B.; Marques, E. C.; Sandstrom, D. R.; Via, G. H.; Sinfelt, J. H. *J. Catal.* **1985**, *95*, 546.
(32) Nardo, S. D.; Lozzi, L.; Passacantando, M.; Picozzi, P.; Santucci, S.; Crescenzi, M. D. *Surf. Sci.* **1994**, *307*−309, 922.
(33) Boyanov, B. I.; Morrison, T. I. *J. Phys. Chem.* **1996**, *100*, 16318.
(34) Masel, R. I. *Principles of Adsorption and Reaction on Solid Surfaces*; John Wiley & Sons, Inc.: New York, 1996.
(35) Gomer, R. In *Solid State Physics: Advances in Research and Applications*; Ehrenreich, H., Seitz, F., Turnbull, D., Eds.; Academic Press: New York, 1975.